Operation of Tracking Circulators

JOSEPH HELSZAJN, MEMBER, IEEE

***Abstract*— The classic two circulation conditions of a junction circulator obtained by setting the imaginary part of the complex gyrator impedance to zero and evaluating the real part does not ensure that the in-phase and counter-rotating eigennetworks are separately idealized. This paper indicates that the physical and magnetic variables of the tracking circulator described by Wu and Rosenbaum coincides with these special boundary conditions. Specifically, the gyrator resistance for this circulator may be calculated at the frequency for which the in-phase eigennetwork exhibits a short-circuit boundary condition (using the $n=0$ and ± 3 modes) and the counter-rotating eigennetwork modes exhibit complex conjugate immittances (using the $n=-1,+2$ and $n=+1,-2$ modes). The paper includes a new formulation for the Q-factor of this type of circulator which is used to calculate that of the tracking circulator.**

I. Introduction

IT IS NOW recognized that the physical and magnetic variables used in the design of many octave band circulators are compatible with the tracking interval defined in the computer study by Wu and Rosenbaum of the Davies and Cohen analysis of stripline circulators [1]–[5]. However, the physical basis for this type of circulator has not yet been described. The purpose of this paper is to remedy this situation by formulating an eigennetwork description of this type of circulator.

The boundary conditions of a symmetrical three-port junction circulator may be either described in terms of its scattering, impedance, or admittance matrices, or in terms of the corresponding reflection, impedance, or admittance eigenvalues. The three sets of eigenvalues are the one-port variables of three one-port networks known as the eigennetworks of the junction. A physical understanding of the junction requires the identification of the eigenvalue problem. In a circulator, using a weakly magnetized resonator, the in-phase eigennetwork is adequately described by the $n=0$ mode (although it is often idealized by a frequency independent short-circuit) and the counter-rotating ones by the $n=+1$ and -1 modes. The eigennetworks for this type of circulator are illustrated in Fig. 1.

The eigenvalue problem for which the eigennetworks require single resonator modes for their description is readily extended to the situation for which higher order modes are necessary by recognizing that they may be realized in a first Foster form expansion of the resonator modes. Using the rotational properties of the eigenvectors it is possible, by inspection, to distribute the resonator modes among the counter-rotating and in-phase eigennetworks. This notation has the advantage that existing literature which has been formulated in terms of eigennetworks supporting single resonator modes is readily extended to the case where higher order modes are required to satisfy the boundary conditions at the junction terminals.

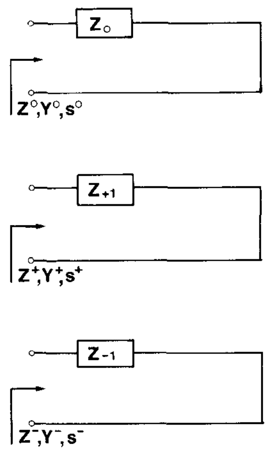

Fig. 1. Eigennetworks of stripline circulator with off-diagonal entry K of tensor permeability in vicinity of zero.

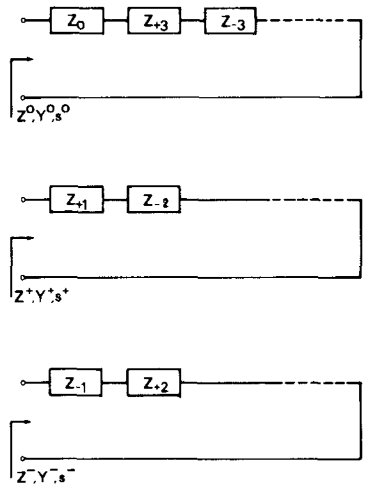

Fig. 2. Eigennetworks of stripline circulator with off diagonal entry K of tensor permeability in tracking region.

The main result of this paper is that the Wu and Rosenbaum first circulation condition coincides with the frequency at which the two counter-rotating eigennetworks exhibit complex conjugate immittances and the in-phase eigennetwork may be idealized by a nearly frequency independent short-circuit. This boundary condition is satisfied by describing the eigenvalue of the in-phase eigennetwork in terms of the $n=0$, ± 3 modes and those of the counter-rotating ones in terms of the $n=+1,-2$ and $n=-1,+2$

Manuscript received September 25, 1980; revised December 23, 1980.

The author is with the Department of Electrical and Electronic Engineering, Heriot-Watt University, 31-35 Grassmarket, Edinburgh EH1 2HT, Scotland.

0018-9480/81/0700-0700$00.75 ©1981 IEEE

modes. The second circulation condition merely involves the calculation of the gyrator resistance using the counter-rotating eigenvalues. The eigennetworks for this type of circulator is depicted in Fig. 2.

A new expression for the loaded Q-factor of junction circulators, which can be described in terms of two complex conjugate counter-rotating eigenvalues with the third, in-phase eigenvalue idealized by a nearly frequency independent short-circuit, is also given.

II. Eigenvalues of Tracking Circulator

In order to study the influence of the different modes of the disk resonator on the Wu and Rosenbaum tracking solution (as a preamble to formulating an analytical solution), it is helpful to segregate the in-phase and counter-rotating junction modes between the eigenvalues of the junction. Inspection of the electromagnetic problem indicates that this may be done by realizing the junction eigennetworks in a first Foster form (rather than in a second Foster form) one-port reactance network in the manner illustrated in Fig. 3. This notation has also been mentioned in [11]

$$Z^0=\sum Z_n, \qquad n=0, \pm 3, \pm 6, \pm 9, \text{etc.} \tag{1}$$

$$Z^+=\sum Z_n, \qquad n=+1, -2, +4, -5, +7, \text{etc.} \tag{2}$$

$$Z^-=\sum Z_n, \qquad n=-1, +2, -4, +5, -7, \text{etc.} \tag{3}$$

This notation has the advantage that once the required terms in each summation have been determined, the other eigenvalues and matrix relations are readily evaluated in the normal way. Thus

$$Y^q=\frac{1}{Z^q} \tag{4}$$

$$s^q=\frac{1-Y^q}{1+Y^q} \tag{5}$$

with $q=0,+,-$.

The open circuit impedance parameters of the three-port junction are readily expanded in terms of (1)–(3) as

$$Z_{11}=\frac{Z^0+Z^++Z^-}{3} \tag{6}$$

$$Z_{12}=\frac{Z^0+Z^+\exp(j2\pi/3)+Z^-\exp(-j2\pi/3)}{3} \tag{7}$$

$$Z_{13}=\frac{Z^0+Z^+\exp(-j2\pi/3)+Z^-\exp(j2\pi/3)}{3}. \tag{8}$$

These impedance parameters are used to express the complex gyrator impedance of the circulator in (18). (The admittance matrix does not normally exist in the case of a stripline circulator.)

The poles of Z^+, Z^-, and Z^0 are defined by the coupling angle ψ and the thickness H of each resonator by

$$Z_n=\frac{j3\sqrt{\mu_{\text{eff}}}\,R_f\sin^2 n\psi}{n^2\pi\psi}\left[\frac{1}{\dfrac{J_{n-1}(kR)}{J_n(KR)}-n\left(\dfrac{1+K/\mu}{kR}\right)}\right] \tag{9}$$

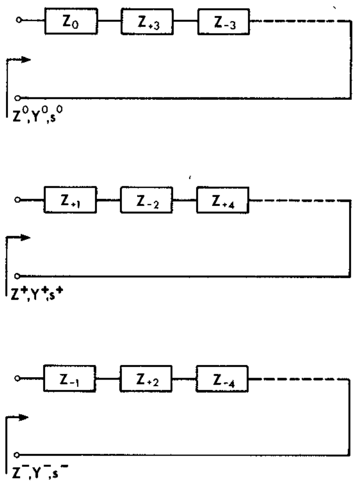

Fig. 3. First Foster form realization of eigennetworks of three-port junction circulator.

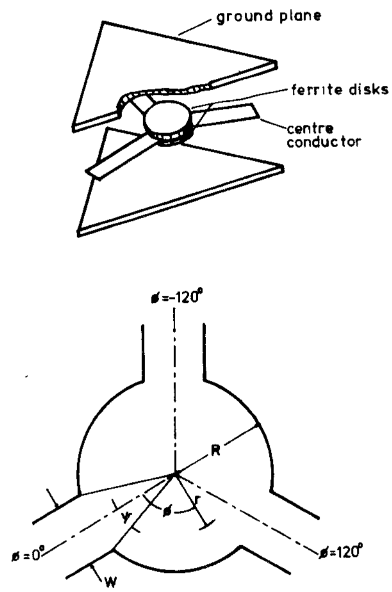

Fig. 4. Schematic diagram of planar junction circulator using disk resonator.

where

$$R_f=\frac{R_r}{\sqrt{\epsilon_f}} \tag{10}$$

$$R_r=\left[30\pi\ln\left(\frac{W+t+2H}{W+t}\right)\right] \tag{11}$$

$$k=\frac{2\pi\sqrt{\epsilon_f\mu_{\text{eff}}}}{\lambda_0} \tag{12}$$

$$\sin\psi=\frac{W}{2R} \tag{13}$$

and the other variables have the usual meaning. Fig. 4 depicts the schematic diagram of the classic planar circulator using a simple disk resonator discussed in this paper.

An essential requirement for the operation of the tracking circulator is that the ferrite material must be saturated.

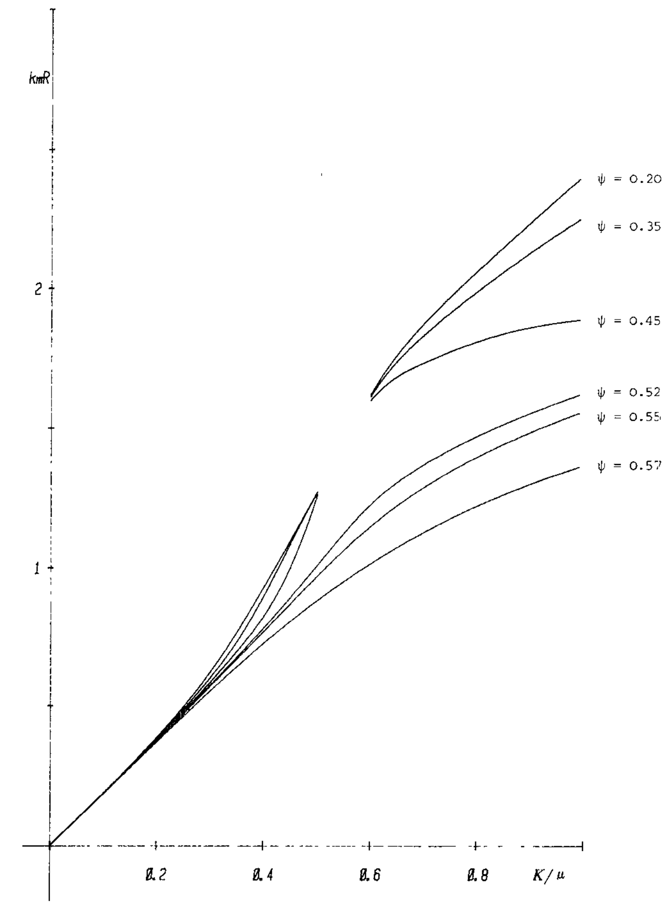

Fig. 5. First circulation solution of junction circulator using disk resonator.

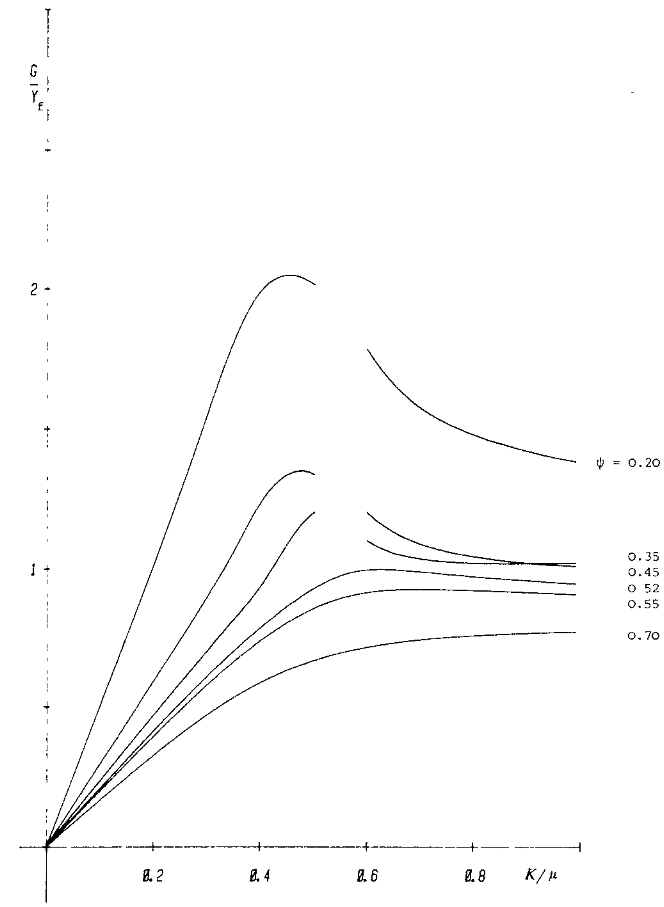

Fig. 6. Second circulation solution of junction circulator using disk resonator.

Thus

$$\frac{K}{\mu}=K=\frac{\omega_m}{\omega} \tag{14}$$

$$\mu_{\text{eff}}=1-K^2=1-\left(\frac{\omega_m}{\omega}\right)^2 \tag{15}$$

where

$$\omega_m=\frac{\gamma M_0}{\mu_0}$$

$\gamma=2.21\times10^5$ (rad/s)/(A/m), M_0 is in tesla, ω is in radians/second, $\mu_0=4\pi\times10^{-7}$ H/m, and $\mu=1$ in a saturated material.

Making use of (14) and (15) allows (12) to be expressed as

$$k=\left(\frac{\omega_m\sqrt{\epsilon_f\mu_{\text{eff}}}}{cK}\right)=k_m\frac{\sqrt{\epsilon_f\mu_{\text{eff}}}}{K} \tag{16}$$

where $k_m=\omega_m/c$, and c is the free space velocity.

The gyrator impedance of the circulator is

$$Z_{\text{in}}=Z_{11}-\frac{Z_{12}^2}{Z_{13}}. \tag{17}$$

This last equation is obtained by writing $V_3=I_3=0$ in obtaining Z_{in} in terms of the open-circuit parameters in (6)–(8).

In what follows, it is useful to express (17) in terms of the eigenvalues in (1)–(3). The result is

$$Z_{\text{in}}=\frac{jB(B^2-3A^2)}{3(A^2+B^2)}+\left[Z^0+\frac{A(B^2-3A^2)}{3(A^2+B^2)}\right] \tag{18}$$

where

$$A=\frac{-1}{2}(Z^++Z^-)+Z^0 \tag{19}$$

$$B=\frac{\sqrt{3}}{2}(Z^+-Z^-). \tag{20}$$

Since the eigenvalues Z^0, Z^-, and Z^+ are pure imaginary numbers, the imaginary part of (18) is the gyrator resistance, and the real part of (18) is the reactance part of Z_{in}.

Figs. 5 and 6 illustrate the two standard circulation conditions [2], [5], [8] obtained by retaining the first seven terms in the partial fraction expansion of the eigenvalues ($n=0,\pm1,\pm2,\pm3$) in (18) according to the scheme in (1)–(3). The illustrations are obtained by setting the imaginary part of the standard complex gyrator impedance (or admittance) in (17) or (18), equal to zero and computing the corresponding real part.

The classic circulation solution is approximately defined by $|K/\mu|$ in the interval 0 to 0.30 on these illustrations (with ψ variable) and its three eigennetworks support the

TABLE I

K/μ	ψ	kR	R	X'	G	B'	Q
0.10	0.54275	1.83705	$5.00558R_f$	$-33.61999R_f$	$0.19978Y_f$	$1.34180Y_f$	6.71650
0.20	0.54485	1.82377	$2.53812R_f$	$-7.83218R_f$	$0.39399Y_f$	$1.21553Y_f$	3.08518
0.30	0.54730	1.79836	$1.73658R_f$	$-3.05901R_f$	$0.57584Y_f$	$1.01435Y_f$	1.76151
0.40	0.54827	1.75499	$1.35864R_f$	$-1.40112R_f$	$0.73603Y_f$	$0.75903Y_f$	1.03126
0.50	0.54487	1.68383	$1.15898R_f$	$-0.66382R_f$	$0.86283Y_f$	$0.49419Y_f$	0.57276
0.60	0.53439	1.57271	$1.05556R_f$	$-0.30946R_f$	$0.94736Y_f$	$0.27773Y_f$	0.29317
0.67	0.52244	1.46503	$1.01805R_f$	$-0.18029R_f$	$0.98227Y_f$	$0.17395Y_f$	0.17709
0.70	0.51634	1.41029	$1.00785R_f$	$-0.14356R_f$	$0.99221Y_f$	$0.14133Y_f$	0.14244
0.80	0.49280	1.18332	$0.98979R_f$	$-0.07063R_f$	$1.01032Y_f$	$0.07208Y_f$	0.07135
0.90	0.46632	0.85524	$0.98508R_f$	$-0.04056R_f$	$1.01515Y_f$	$0.04179Y_f$	0.04117
0.95	0.45257	0.61054	$0.98469R_f$	$-0.03357R_f$	$1.01555Y_f$	$0.03462Y_f$	0.03409

$n=0$, $+1$, and -1 resonances of the disk resonator. These are the Bosma [6] and Fay and Comstock [7] solutions. The Wu and Rosenbaum tracking solution requires the $n=0$, ± 1, ± 2, and ± 3 modes for its description and operates with the magnetic variable $|K|$ between 0.5 and 1 with $\psi \approx 0.55$ but no closed form solution is available for it. For $0 \leqslant \psi \leqslant 0.50$, the solution of $k_m R$ is ill defined for $K/\mu \approx 0.50$, and this region is left blank in Figs. 5 and 6.

III. Three Eigennetwork Theory of Tracking Circulator

This section shows that the first Wu and Rosenbaum boundary condition coincides with the frequency at which the two counter-rotating eigennetworks exhibit complex conjugate immittances, and the in-phase eigennetwork may be idealized by a short-circuit boundary condition. The second boundary condition is shown to be approximately satisfied by assuming that the counter-rotating eigennetworks support the $n=+1$, -2 and $n=-1$, $+2$ resonator modes.

The first boundary condition may be demonstrated by simultaneously satisfying

$$Z^0 = Z_0 + Z_{+3} + Z_{-3} = 0 \tag{21}$$

and

$$Z^+ + Z^- = (Z_{+1} + Z_{-2}) + (Z_{-1} + Z_{+2}) = 0. \tag{22}$$

The first equation ensures that Z^0 satisfies a short-circuit boundary condition at the input terminals of the device, and the second one ensures that the operating frequency coincides with that at which the two counter-rotating eigennetworks exhibit complex conjugate immittances. The simultaneous solution of (21) and (22) is a unique solution to (18). The first 7 entries in Table I give the required result over the whole field of variables. It is apparent from this data that the Wu and Rosenbaum solution given by $\psi \approx 0.522$ rad, $K \approx 0.67$, and $kR \approx 1.465$ is a solution to the boundary conditions expressed by (21) and (22). Thus their first circulation solution is compatible with the three eigennetwork theory described by (21) and (22).

Since it may occasionally be useful to construct tracking circulators with narrow coupling angles it is desirable to be able to independently adjust the in-phase eigennetwork. One independent variable that allows Z_0 to be tuned without perturbing the other resonator modes is a thin metal post through the centre of the resonator. The form of Z_0 in (21) is readily shown to take the following form:

$$Z_0 = \frac{-j3\sqrt{\mu_{\text{eff}}}\,R_f \psi}{\pi}\left[\frac{J_0(kR)Y_0(ka) - J_0(ka)Y_0(kR)}{J_1(kR)Y_0(ka) - J_0(ka)Y_1(kR)}\right] \tag{23}$$

where $Y_0(x)$ and $Y_1(x)$ are Bessel functions of the second kind, and a is the radius of the metal post. Evaluation of (21) and (22) with ka as a parameter indicates that introducing such a metal post thru the centre of the junction does indeed lead to a reduction in the coupling angle ψ.

Once the first circulation (frequency) is satisfied, the second one (gyrator level) may be calculated by having recourse to the real part of (18)

$$R_{\text{in}} = j\left(\frac{Z^+ - Z^-}{2\sqrt{3}}\right) \tag{24}$$

where

$$Z^+ \approx Z_{+1} + Z_{-2}$$
$$Z^- \approx Z_{-1} + Z_{+2}.$$

Evaluating Z_n using (9) with $\psi = 0.52244$, $kR = 1.46503$, and $K/\mu = 0.67$, yields

$$Z_{+1} = -j1.88869R_f$$
$$Z_{-1} = +j0.45920R_f$$
$$Z_{+2} = +j1.30413R_f$$
$$Z_{-2} = +j0.12537R_f.$$

Thus

$$Z^+ = -j1.76332R_f$$
$$Z^- = +j1.76333R_f$$
$$R_{\text{in}} = 1.01805R_f$$

in agreement with the appropriate entry in column 7 of Table I.

Evaluating R_f in (10) with $\epsilon_f = 15.3$, and $R_r = 50\ \Omega$ gives the gyrator resistance of the circulator as

$$R_{\text{in}} = 13.00\ \Omega.$$

For completeness the magnitudes of the in-phase eigenvalues in (31) are

$$Z_0 = -j0.35593R_f$$
$$Z_{+3} = +j0.30928R_f$$

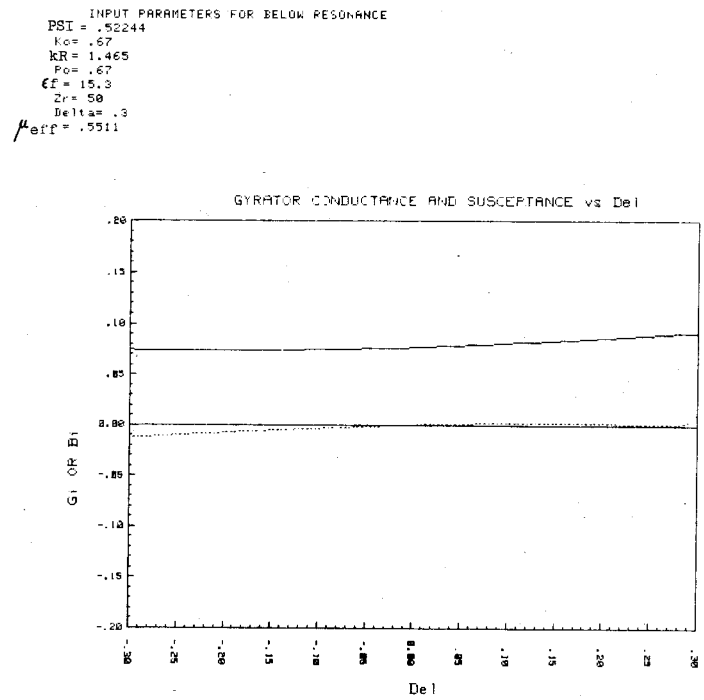

Fig. 7. Variation of real and imaginary parts of tracking circulator with $K/\mu = 0.67$, $kR = 1.46$, $\psi = 0.522$.

TABLE II

K/μ	X_0	X_3	X_{-3}	X_1	X_{-1}	X_2	X_{-2}	X^0	X^+	X^-
0.10	$-0.28222R_f$	$0.15766R_f$	$0.12457R_f$	$-9.06443R_f$	$8.14300R_f$	$0.52731R_f$	$0.39490R_f$	$0.00001R_f$	$-8.66952R_f$	$8.67031R_f$
0.20	$-0.28579R_f$	$0.17631R_f$	$0.10948R_f$	$-4.73723R_f$	$3.78262R_f$	$0.61383R_f$	$0.34138R_f$	$0.00001R_f$	$-4.39585R_f$	$4.39645R_f$
0.30	$-0.29232R_f$	$0.19718R_f$	$0.09514R_f$	$-3.30063R_f$	$2.28703R_f$	$0.72062R_f$	$0.29257R_f$	$0.00000R_f$	$-3.00806R_f$	$3.00765R_f$
0.40	$-0.30274R_f$	$0.22126R_f$	$0.08149R_f$	$-2.59950R_f$	$1.50043R_f$	$0.85289R_f$	$0.24637R_f$	$0.00000R_f$	$-2.35313R_f$	$2.35332R_f$
0.50	$-0.31822R_f$	$0.24978R_f$	$0.06844R_f$	$-2.20853R_f$	$0.99628R_f$	$1.01113R_f$	$0.20113R_f$	$0.00000R_f$	$-2.00740R_f$	$2.00740R_f$
0.60	$-0.33904R_f$	$0.28334R_f$	$0.05570R_f$	$-1.98450R_f$	$0.64364R_f$	$1.18467R_f$	$0.15623R_f$	$-0.00001R_f$	$-1.82826R_f$	$1.82831R_f$
0.67	$-0.35593R_f$	$0.30928R_f$	$0.04666R_f$	$-1.88869R_f$	$0.45920R_f$	$1.30413R_f$	$0.12537R_f$	$0.00001R_f$	$-1.76332R_f$	$1.76333R_f$
0.70	$-0.36345R_f$	$0.32075R_f$	$0.04270R_f$	$-1.85805R_f$	$0.39285R_f$	$1.35282R_f$	$0.11243R_f$	$0.00000R_f$	$-1.74562R_f$	$1.74567R_f$
0.80	$-0.38835R_f$	$0.35932R_f$	$0.02903R_f$	$-1.78553R_f$	$0.21571R_f$	$1.49864R_f$	$0.07114R_f$	$-0.00001R_f$	$-1.71439R_f$	$1.71435R_f$
0.90	$-0.41109R_f$	$0.39641R_f$	$0.01469R_f$	$-1.73975R_f$	$0.09017R_f$	$1.61598R_f$	$0.03349R_f$	$0.00000R_f$	$-1.70626R_f$	$1.70616R_f$
0.95	$-0.42113R_f$	$0.41378R_f$	$0.00736R_f$	$-1.72181R_f$	$0.04146R_f$	$1.66401R_f$	$0.01621R_f$	$0.00001R_f$	$-1.70560R_f$	$1.70547R_f$

and

$$Z_{-3} = +j0.04666R_f.$$

Thus

$$Z^0 = 0.$$

The eigenvalues and poles at the circulation conditions are tabulated in Table II.

Fig. 7 indicates the variation of the real and imaginary parts of Z_{in} with frequency for this boundary condition and shows that its equivalent circuit is well behaved as asserted. It is also observed that the loaded Q-factor obtained graphically from Fig. 7 is in excellent agreement with the value tabulated in Table I.

IV. Susceptance Slope Parameter and Loaded Q-Factor of Three Eigennetwork Junction Circulators

A complete description of a junction circulator also requires a knowledge of the susceptance slope parameter and loaded Q-factor of the complex gyrator network. These two quantities will now be determined in this section. Good agreement is obtained between the closed-form expressions in this section and a separate numerical computation.

The derivation starts by expressing the imaginary part of the input impedance in terms of its real part by rewriting (18) in the following form:

$$Z_{\text{in}} = R_{\text{in}} + \left(Z^0 - j\frac{AR_{\text{in}}}{B} \right) \tag{25}$$

where

$$R_{\text{in}} = j\frac{B(B^2 - 3A^2)}{3(A^2 + B^2)} \tag{26}$$

$$jX_{\text{in}} = Z^0 - j\frac{AR_{\text{in}}}{B}. \tag{27}$$

Idealizing the in-phase eigennetwork in describing R_{in} leads to

$$R_{\text{in}} = j\frac{B}{3} = j\frac{(Z^+ - Z^-)}{2\sqrt{3}}. \tag{28}$$

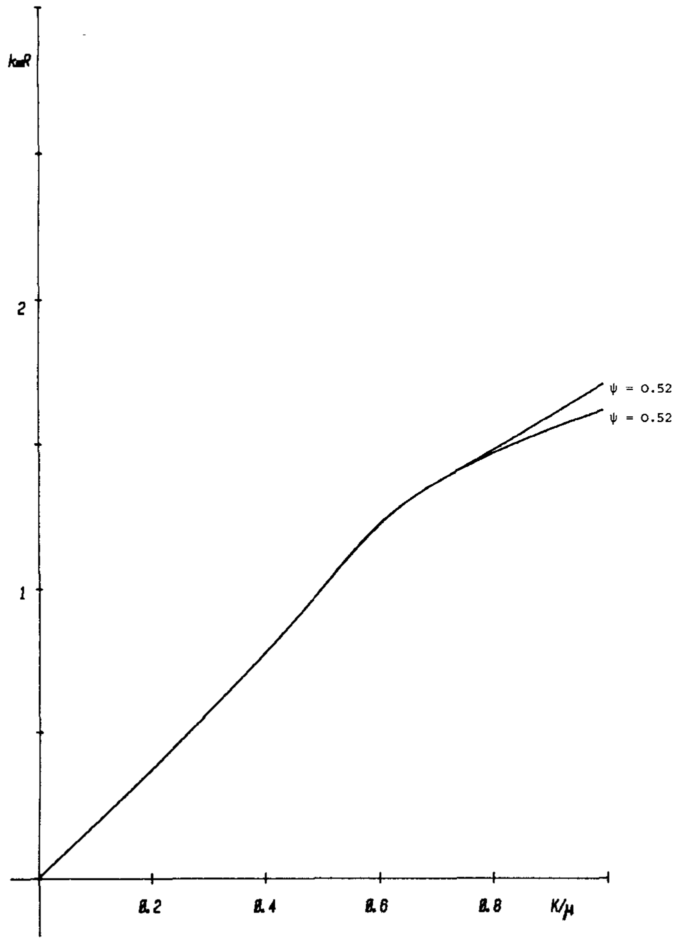

Fig. 8. Comparison between exact and approximate first circulation solution for disk resonator.

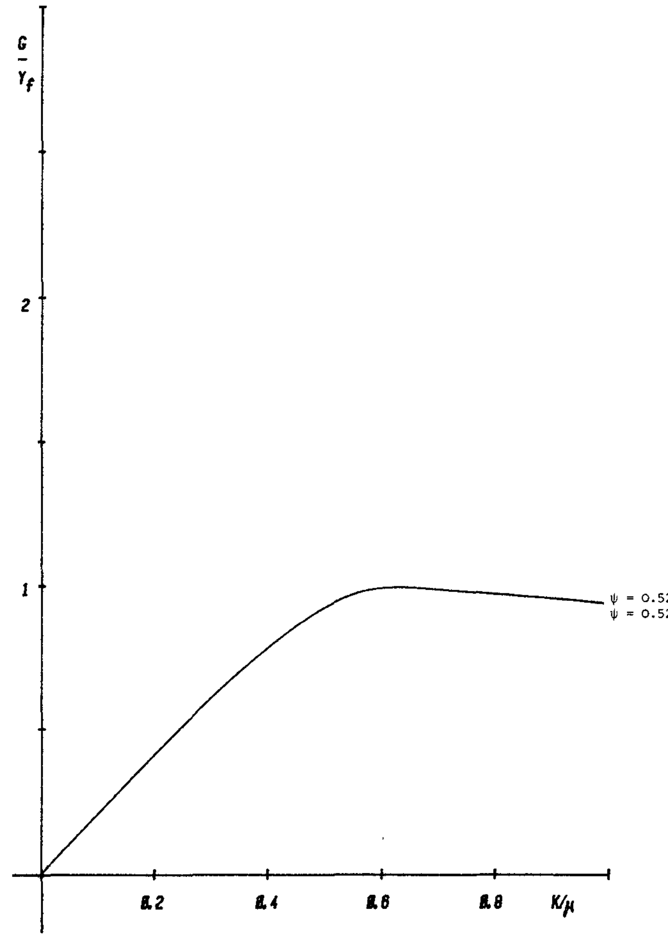

Fig. 9. Comparison between exact and approximate second circulation solution for junction circulator using disk resonator.

An approximate three eigennetwork description of the imaginary part of Z_{in} is now obtained by substituting (19) and (28) into (27). The result is

$$jX_{in} = Z^0 + \frac{A}{3}$$

$$= \frac{8Z^0 - (Z^+ + Z^-)}{6} \tag{29}$$

The agreement between the two circulation conditions for $\psi = 0.52$ using the real and imaginary parts in (28) and (29) and the exact functions in (18) are depicted in Figs. 8 and 9.

Since both R_{in} and X_{in} involve the difference between positive real functions (Z^0, Z^+, Z^-), neither R_{in} or X_{in} in (28) and (29) need be positive real functions. This suggests that it may not be possible to realize Z_{in} in terms of basic LCR elements. The sign of R_{in} merely indicates the direction of circulation of the device and poses no difficulty. However, if X_{in} is not a reactance function, it is not realizable in terms of LC elements. This situation arises if $8Z^0 \leqslant (Z^+ + Z^-)$ in (29). Taking the conventional boundary condition in which Z^0 is assumed zero indicates that X_{in} is not a reactance function, but that the imaginary part of Y_{in} is a susceptance function. This suggests that a shunt network is often the preferred equivalent circuit of junction circulators.

Forming Y_{in} gives

$$Y_{in} = \frac{1}{Z_{in}} = \frac{R_{in} - \left[\frac{8Z^0 - (Z^+ + Z^-)}{6}\right]}{R_{in}^2 + \left[\frac{8Z^0 - (Z^+ + Z^-)}{6}\right]^2}. \tag{30}$$

For $R_{in}^2 \gg \left[\frac{8Z^0 - (Z^+ + Z^-)}{6}\right]^2$

$$G_{in} \approx \frac{1}{R_{in}} \tag{31}$$

$$jB_{in} \approx \frac{-\left[8Z^0 - (Z^+ + Z^-)\right]}{6R_{in}^2}. \tag{32}$$

The susceptance slope parameter is seen to be a positive susceptance function provided Z^0 is zero or $Z^0 \leqslant (Z^+ + Z^-)$. Equations (28), (29), (31), and (32) yield compatible conductance/resistance and frequency conditions.

It is observed that the reactance and susceptance slope parameters X' and B' are related by

$$B'_{in} = \frac{-X'_{in}}{R_{in}^2} \tag{33}$$

TABLE III

K/u	X'_0	X'_3	X'_{-3}	X'_1	X'_{-1}	X'_2	X'_{-2}	$X^{0'}$	$X^{+'}$	$X^{-'}$	X'
0.10	$0.47780R_f$	$0.10250R_f$	$0.09039R_f$	$105.45605R_f$	$100.72021R_f$	$0.51834R_f$	$0.39087R_f$	$0.67069R_f$	$105.84692R_f$	$101.23855R_f$	$-33.61999R_f$
0.20	$0.48163R_f$	$0.11104R_f$	$0.08605R_f$	$27.09096R_f$	$24.35918R_f$	$0.62234R_f$	$0.35033R_f$	$0.67872R_f$	$27.44129R_f$	$24.98152R_f$	$-7.83218R_f$
0.30	$0.48693R_f$	$0.12211R_f$	$0.08254R_f$	$12.52721R_f$	$10.26921R_f$	$0.77197R_f$	$0.31822R_f$	$0.69157R_f$	$12.88543R_f$	$11.04118R_f$	$-3.05901R_f$
0.40	$0.49176R_f$	$0.13655R_f$	$0.07981R_f$	$7.48299R_f$	$5.31026R_f$	$0.98748R_f$	$0.29097R_f$	$0.70812R_f$	$7.77396R_f$	$6.29773R_f$	$-1.40112R_f$
0.50	$0.49292R_f$	$0.15505R_f$	$0.07789R_f$	$5.24523R_f$	$2.99500R_f$	$1.28388R_f$	$0.26564R_f$	$0.72586R_f$	$5.51087R_f$	$4.27888R_f$	$-0.66382R_f$
0.60	$0.48732R_f$	$0.17734R_f$	$0.07678R_f$	$4.13306R_f$	$1.76663R_f$	$1.64806R_f$	$0.24057R_f$	$0.74145R_f$	$4.37364R_f$	$3.41469R_f$	$-0.30946R_f$
0.67	$0.47907R_f$	$0.19429R_f$	$0.07632R_f$	$3.68601R_f$	$1.25372R_f$	$1.91612R_f$	$0.22333R_f$	$0.74968R_f$	$3.90933R_f$	$3.16984R_f$	$-0.18029R_f$
0.70	$0.47462R_f$	$0.20164R_f$	$0.07616R_f$	$3.54472R_f$	$1.09162R_f$	$2.02823R_f$	$0.21614R_f$	$0.75242R_f$	$3.76085R_f$	$3.11985R_f$	$-0.14356R_f$
0.80	$0.45733R_f$	$0.22556R_f$	$0.07561R_f$	$3.20994R_f$	$0.71844R_f$	$2.36981R_f$	$0.19356R_f$	$0.75849R_f$	$3.40350R_f$	$3.08825R_f$	$-0.07063R_f$
0.90	$0.43827R_f$	$0.24735R_f$	$0.07481R_f$	$2.99873R_f$	$0.50722R_f$	$2.64717R_f$	$0.17374R_f$	$0.76043R_f$	$3\ 17248R_f$	$\cdot 3.15439R_f$	$-0.04056R_f$
0.95	$0.42863R_f$	$0.25709R_f$	$0.07424R_f$	$2.91848R_f$	$0.43718R_f$	$2.76050R_f$	$0.16489R_f$	$0.75995R_f$	$3.08337R_f$	$3\ 19768R_f$	$-0.03357R_f$

provided it is assumed that R_{in} is essentially frequency independent.

Finally, the loaded Q-factor of the network is obtained from either circuit descriptions

$$Q_L = \frac{-X'_{\text{in}}}{R_{\text{in}}} = \frac{B'_{\text{in}}}{G_{\text{in}}} \tag{34}$$

as is readily verified. It is obvious from (29) and (32) that X_{in} or B_{in} are strongly dependent upon the in-phase eigenvalue.

The reactance slope parameter of the tracking circulator may now be readily obtained by forming

$$X'_{\text{in}} = \frac{\omega_0}{2} \cdot \frac{dX_{\text{in}}}{d\omega}\bigg|_{\omega=\omega_0}. \tag{35}$$

X_{in} is defined in (29) and ω_0 is the frequency at which X_{in} is zero

$$X_{\text{in}} = \frac{8X^0 - (X^+ + X^-)}{6}. \tag{36}$$

Since X_{in} is a linear combination of X_n in (9), X'_{in} may be evaluated once the reactance slope parameter X'_n below is determined

$$X'_n = \frac{\omega}{2} \cdot \frac{dX_n}{d\omega}\bigg|_{\omega_0} = \frac{\omega}{2}\left[\frac{\delta X_n}{\delta\sqrt{\mu_{\text{eff}}}} \cdot \frac{\delta\sqrt{\mu_{\text{eff}}}}{\delta\omega} + \frac{\delta X_n}{\delta K} \cdot \frac{\delta K}{\delta\omega} + \frac{\delta X_n}{\delta kR} \cdot \frac{\delta kR}{\delta\omega}\right]_{\omega_0}. \tag{37}$$

X_n is given in (9) by

$$X_n = \frac{T_n\sqrt{\mu_{\text{eff}}}}{\dfrac{J_{n-1}(kR)}{J_n(kR)} - n\left(\dfrac{1+K}{kR}\right)} \tag{38}$$

where

$$T_n = \frac{3R_f \sin^2 n\psi}{n^2\pi\psi} \tag{39}$$

K, μ_{eff}, and kR are defined in terms of ω in (12), (14), and (15). The result for the partial derivatives is

$$\omega\frac{\delta X_n}{\delta\sqrt{\mu_{\text{eff}}}}\frac{\delta\sqrt{\mu_{\text{eff}}}}{\delta\omega} = X_n\left(\frac{K^2}{1-K^2}\right) \tag{40}$$

$$\omega\frac{\delta X_n}{\delta K}\frac{\delta K}{\delta\omega} = -X_n^2\left(\frac{nK}{T_n kR(1-K^2)^{1/2}}\right) \tag{41}$$

$$\omega\frac{\delta X_n}{\delta kR}\frac{\delta kR}{\delta\omega} = \frac{T_n kR}{(1-K^2)^{1/2}} + \frac{X_n}{(1-K^2)}(1-2nK) + \frac{X_n^2}{T_n kR(1-K^2)^{3/2}}\left[-n^2(1-K^2)+(kR)^2\right]. \tag{42}$$

The reactance slope parameter in (35) has been computed and is displayed in Table III. In keeping with the earlier remarks, the equivalent circuit is also formulated in Table I in terms of G and B' in (31) and (32). For completeness, the loaded Q-factor obtained from either statements in (34) is also tabulated in this table.

In the nontracking region, G, B', and Q_L approximately satisfy the classic Bosma functions with $0 \leq K/\mu \leq 0.30$ as is readily verified

$$G_{\text{in}} = \frac{\pi Y_f}{\sqrt{3}\sqrt{\mu_{\text{eff}}}(kR)\sin\psi}\frac{K}{\mu} \tag{43}$$

$$B_{\text{in}} = \frac{\pi Y_f}{3\sqrt{\mu_{\text{eff}}}\sin\psi}\left[\frac{J'_1(kR)}{J_1(kR)}\right] \tag{44}$$

$$B'_{\text{in}} = \frac{\pi Y_f}{3\sqrt{\mu_{\text{eff}}}\sin\psi}\left[\frac{(kR)^2-1}{2kR}\right] \tag{45}$$

$$Q_L = \left[\frac{(kR)^2-1}{2\sqrt{3}}\right]\frac{\mu}{K} \tag{46}$$

with $kR = 1.84$.

In the tracking region, Q_L is small but not zero. A solution with Q_L zero, in the neighborhood of the first circulation condition may very likely be obtained by setting X'_{in} in (35) to zero, but this has not been done at this time.

V. Conclusions

This paper has described a simple new formulation of junction circulators for which the operating frequency coincides with that at which the in-phase eigennetwork can be idealized by a short-circuit boundary condition and the counter-rotating eigennetworks exhibit complex conjugate immittances. Also included is the loaded Q-factor for this type of junction. It is further demonstrated that the Wu and Rosenbaum tracking circulator belongs to this type of device. The agreement between the closed form expression for the loaded Q-factor of the junction and a numerical calculation are in excellent agreement.

ACKNOWLEDGMENT

The author would like to thank Hugh Conner of Heriot-Watt University for the computations in this paper.

REFERENCES

[1] J. W. Simon, "Broadband strip-transmission line Y-junction circulators," *IEEE Trans. Microwave Theory Tech.*, vol. MTT-13, 335–345, May 1965.
[2] Y. S. Wu and F. J. Rosenbaum, "Wideband operation of microstrip circulators," *IEEE Trans. Microwave Theory Tech.*, vol. MTT-22, pp. 849–856, Oct. 1974.
[3] J. de Koning *et al.*, "Full band low loss continuous tracking circulation in K band," *IEEE Trans. Microwave Theory Tech.*, vol. MTT-25, pp. 152–157, Feb. 1977.
[4] J. Helszajn *et al.*, "Synthesis of stripline circulator using frequency independent real gyrators," *MOA*, to be published.
[5] S. Ayter and Y. Ayasi, "The frequency behaviour of stripline circulator junctions," *IEEE Trans. Microwave Theory Tech.*, vol. MTT-26, pp. 197–202, Mar., 1978.
[6] H. Bosma, "On stripline Y-circulation at UHF," *IEEE Trans. Microwave Theory Tech.*, vol. MTT-12, pp. 61–72, Jan. 1964.
[7] C. E. Fay and R. L. Comstock, "Operation of the ferrite junction circulator," *IEEE Trans. Microwave Theory Tech.*, vol. MTT-13, pp. 15–21, Jan. 1965.
[8] J. B. Davies and P. Cohen, "Theoretical design of symmetrical junction stripline circulators," *IEEE Trans. Microwave Theory Tech.*, vol. MTT-11, pp. 506–512, Nov. 1963.
[9] J. Helszajn, "The synthesis of quarter-wave coupled circulators with Chebyshev characteristics," *IEEE Trans. Microwave Theory Tech.*, vol. MTT-20, pp. 764–769, Nov. 1972.
[10] J. Helszajn, *Nonreciprocal Microwave Junctions and Circulators.* New York: Wiley, 1975.
[11] H. Bosma, "Junction Circulators," *Advances in Microwaves*, vol. 6, pp. 191–194, 219–223, 1971.

Propagation Constant Below Cutoff Frequency in a Circular Waveguide with Conducting Medium

TAKEO ABE, MEMBER, IEEE, AND YOSHIO YAMAGUCHI

***Abstract*—Exact and approximate propagation characteristics of normal modes in the cutoff region of a circular waveguide surrounded by a medium of finite conductivity are discussed. An exact solution is obtained by numerical analysis, and an approximate one is derived by expanding the characteristic equation considering the finite conductivity of the cylinder wall. The computed values are compared with experimental ones. It is shown that the attenuation of TM_{01} mode at frequencies that are much lower than the cutoff frequency is constant, i.e., independent of frequency and the material constants of the external medium, and this mode is the most suitable one for realizing a precision circular piston attenuator.**

I. INTRODUCTION

AT PRESENT, the dominant HE_{11} mode is used for circular piston attenuators operating below cutoff frequency. An approximate propagation theory [1], [2], has been derived for these attenuators under the assumption that the conductivity of the cylinder wall is infinite. The attenuation of the HE_{11} mode, by this theory, should be constant at frequencies that are much lower than the cutoff frequency. Experimental attenuation values, however, vary with frequency. This phenomenon seems to be caused by the finite conductivity of the guide wall. A correction to the attenuation of the HE_{11} mode has been reported by Brown [3].

Manuscript received October 24, 1980; revised December 10, 1980.
The authors are with the Faculty of Engineering, Niigata University, Niigata, 950-21 Japan.

Obviously, if a mode could be found that is independent of frequency and conductivity, an ideal attenuator could be realized based on this mode. For these reasons, we investigated several modes of circular waveguide, taking into consideration the finite conductivity of the guide wall.

This paper reports the propagation characteristics of normal modes in the cutoff region of a circular waveguide surrounded by a medium of finite conductivity. Exact and approximate propagation constants are derived, experimental values are presented, the distribution of E_z in the radial direction is discussed, and the ideal mode for a precision circular piston attenuator is pointed out.

II. CHARACTERISTIC EQUATION

A hollow circular cylinder of radius a and of infinite length is surrounded by a dissipative medium as shown in Fig. 1. No restriction is imposed on the conductivity of the external medium. The normal modes in this cylinder are of four types; circularly symmetric TE_{0m}, TM_{0m}, and hybrid HE_{nm}, EH_{nm} modes which reduce to TE_{nm}, TM_{nm} when the conductivity of the external medium becomes infinite. These modes are assumed to have time and z variation of